ELSEVIER

Available online at www.sciencedirect.com

ScienceDirect

Reliability Engineering and System Safety 00 (2014) 1–17

Reliability Engineering & System Safety

Coupling mode-destination accessibility with a quantitative seismic-risk assessment to identify at-risk communities

Mahalia Miller[a], Jack W. Baker[a]

[a]*Stanford University, Stanford, CA USA*

Abstract

In this paper, we develop a framework for coupling mode-destination accessibility with a quantitative seismic-risk assessment to identify communities at a high risk for travel disruptions after an earthquake. Mode-destination accessibility measures the ability of people to reach destinations they desire; it is calculated as the log value of the sum of a function of the utilities of each destination over all possible destinations and travel modes, where the utility decreases if getting to that destination is more costly or time-intensive. We use a probabilistic seismic risk assessment procedure, including a stochastic set of earthquake events, ground-motion intensity maps, damage maps, and realizations of traffic and accessibility impacts. For a case study of the San Francisco Bay Area, we couple our seismic risk framework with a practical activity-based traffic model. As a result, we quantity accessibility risk probabilistically by community and household type. We find that accessibility varies more strongly as a function of travelers' geographic location than as a function their income class, and we identify particularly at-risk communities. We also observe that communities more conducive to local trips by foot or bike are predicted to be less impacted by losses in accessibility. This work shows the potential to link quantitative risk assessment methodologies with high-resolution travel models used by transportation planners. Quantitative risk metrics of this type should have great utility for planners working to reduce risk to a region's infrastructure systems.

Keywords: Infrastructure, Risk, Earthquakes, Transportation Network, Accessibility

1. Introduction

Seismic risk assessment in earthquake engineering tends to focus on buildings, bridges, and the performance of infrastructure systems. For measuring the performance of transportation systems, researchers typically use engineering-based metrics such as the post-earthquake connectivity loss, which quantifies the decrease in the number of origins or generators connected to a destination node [e.g., 1], or the post-earthquake travel distance between two locations of interest [e.g., 2]. These frameworks have provided insight into seismic vulnerability and possible risk mitigation, but do not directly quantify ramifications for people.

In the field of vulnerability sciences, researchers have long stressed the importance of the impact on human welfare from earthquakes. For example, Bolin and Stanford write that,"'Natural' disasters have more to do with the social, political, and economic aspects than they do with the environmental hazards that trigger them. Disasters occur at the interface of vulnerable people and hazardous environments" [3]. A recent World Bank and United Nations report echoed this idea that the effects on human welfare turn natural hazards into disasters [4].

Historical events emphasize the complex social effects of earthquakes. For example, on one hand the 1994 Northridge earthquake caused major damage to nine bridges, which, while significant, represented only 0.5% of the bridges estimated by Caltrans to have experienced significant shaking [5]. On the other hand, over half of businesses reported closing after the earthquake with 56% citing the "inability of employees to get to work" as a reason [6]. Furthermore, the total economic cost of transport-related interruptions ("commuting, inhibited customer access, and shipping and supply disruptions") from this earthquake is estimated at 2.16 billion USD (2014) [7], using the consumer price index to account for inflation.

Some researchers have measured the impact of earthquakes on transportation infrastructure using the cumulative extra time needed for travel due to damage, sometimes called travel time delay [e.g., 8, 9]. This performance measure captures basic re-routing due to road closures and identifies roads more likely to be congested. Travel time approximately measures impact on people, but does not capture the fact that some destinations and trips have higher value than others. It also focuses on aggregate regional effects rather than individual communities and demographic groups. Others have considered the qualitative criteria-based metric "disruption index" [10], but this does not provide a quantitative link between physical damage to infrastructure and resulting human ramifications. Other work has looked at resiliency, but defined it in pure engineering terms, such as percentage of a road network that is functional [11]. Outside of transportation systems, some researchers have investigated the interplay between earthquake damage, such as damage to the electric power and wastewater networks, and the usability of houses and other buildings [12].

In contrast to the work on transportation-related seismic risk, urban planning has a long tradition of studying the impact on people of events and policy [13]. Accessibility is one metric popular in urban planning to measure the impact of different transportation network scenarios, and it measures how easily people can get to desirable destinations, which is one measure of social impact [14]. Within urban planning, accessibility has been measured in many ways, including individual accessibility, economic benefits of accessibility, and mode-destination accessibility [15]. The mode-destination accessibility is computed by taking the log value of the sum of a function of the utilities of each destination over all possible destinations and travel modes, where the utility decreases if getting to that destination is more costly or time-intensive [16]. This choice of accessibility definition is particularly useful for quantifying the impacts of disasters such as earthquakes, because certain destinations might be more critical for people in certain locations or from different socio-economic groups. However, this accessibility measure has not yet been linked to risk assessment. In addition, the majority of work to date assumes that travel demand and mode choice will remain unchanged after a future earthquake, which historical data suggests is not the case [7]. A first step towards considering variable demand is work in the literature that varies demand by applying a constant multiplicative factor on all pre-earthquake travel demand [8], but again this approach lacks any resolution at the geographic or socio-economic level.

In this paper, we develop a framework for coupling mode-destination accessibility with a quantitative seismic-risk assessment to identify at-risk populations and measure the accompanying impacts on human welfare. We illustrate our approach with a case study of the San Francisco Bay Area transportation network, including highways, local roads, and public transportation lines. This study analyzes a set of forty hazard-consistent earthquake scenarios, ground-motion intensity maps, and damage maps, as introduced in [17] using the optimization procedure proposed in [18]. For each of these damage maps, we model damage with an agent-based transportation model used by the local transportation authorities that considers the impacts of damage to bridges, roads, and transit lines, and captures variable user demand. Then, with this model, we estimate losses in accessibility for 12 socio-economic groups and for a number of communities within the study region.

2. Case study: San Francisco Bay Area

We consider the San Francisco Bay Area to illustrate our approach (Figure 1). This seismically active area follows a polycentric metropolitan form, with San Francisco as the primary center and other jobs concentrated in suburban centers such as Silicon Valley [19]. The region has a wide array of trip patterns for mandatory and non-mandatory trips. Furthermore, trip times and routes vary greatly depending on travel preferences and workplace locations [19]. Thus, there may be noticeable disparities among households in the risk of travel-related impacts due to earthquakes.

This analysis considers the complex web of roads and transit networks of the case study area. The roads are modeled by a directed graph $G = (V, E)$, where V is a finite set of vertices representing intersections, and the set E, whose elements are edges representing road links, is a binary relation on V. In this model, $(|V|, |E|) = (11{,}921, 32{,}858)$ including centroidal links and $(|V|, |E|) = (9{,}635, 24{,}404)$ without. Centroidal links do not correspond to particular physical roads but instead capture flows of people from outside the study area or from some minor local roads. Forty three transit networks such as bus, light rail and ferry systems are also modeled.We model potential

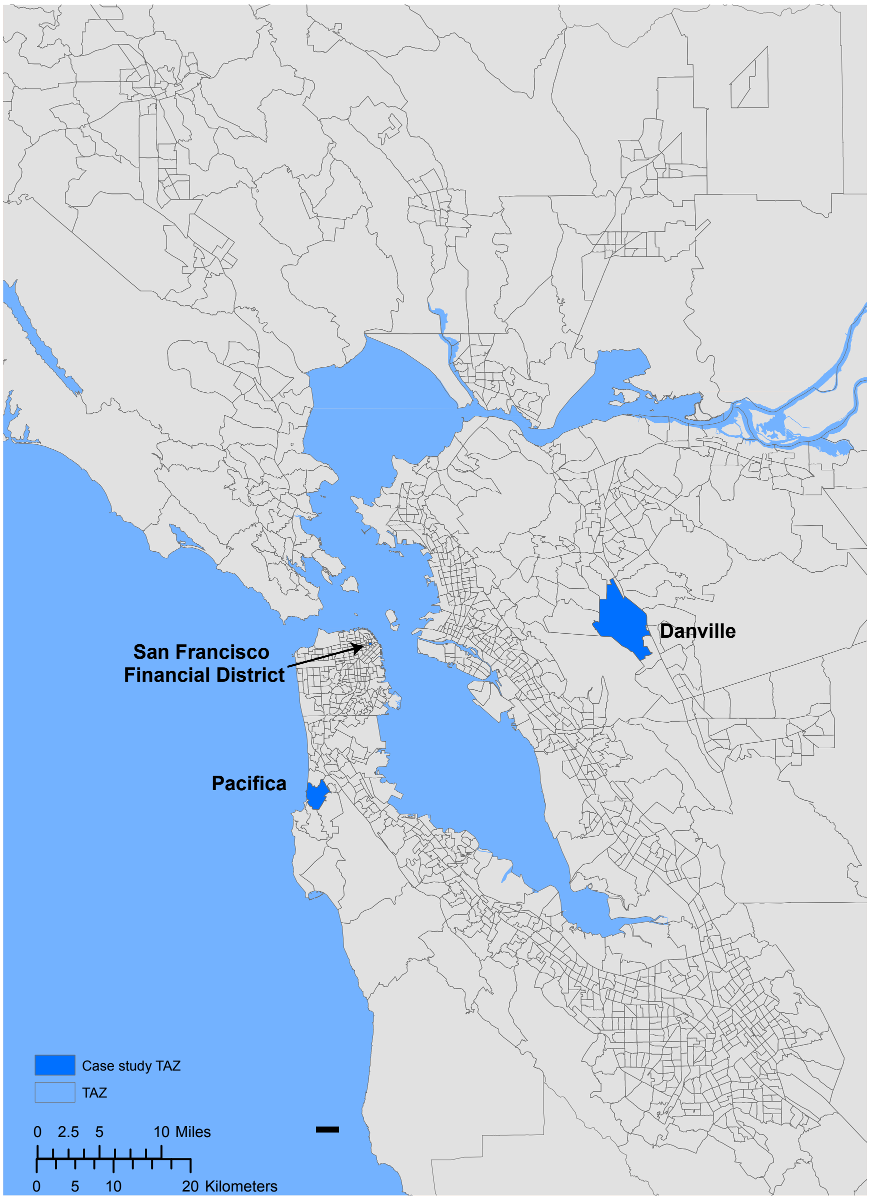

Figure 1. Travel analysis zones (TAZs) in the San Francisco Bay Area. Shading indicates three specific TAZs that are considered in more detail below. **TODO: label cities mentioned in the paper**

damage to 1743 highway bridges impacting the road and some transit networks, and 1409 structures impacting the rapid transit network, BART. Details of the seismic risk calculations for this network are provided in the following subsections.

2.1. Ground-motion intensity maps

2.1.1. Theory

We now describe how to produce a set of maps with ground-motion intensity realizations at each location of interest, and corresponding occurrence rates that reasonably capture the joint distribution of the ground-motion intensity at all locations of interest throughout the region. First, we generate Q earthquake scenarios from a seismic source model, which specifies the rates at which earthquakes of various magnitudes, locations, and faulting types will occur. This set of earthquake scenarios is comparable to a stochastic event catalogue in the insurance industry.

Second, for each earthquake scenario in the seismic source model, we use an empirical ground-motion prediction equation (GMPE) [e.g., 20] to predict the log mean and standard deviation of a ground motion intensity measure at each location of interest. Then, for each of the Q earthquake scenarios, we sample b realizations of spatially correlated ground-motion intensity residual terms [e.g., 26]. The total log ground-motion intensity (Y) for a given realization is computed as

$$\ln Y_{ij} = \overline{\ln Y(M_j, R_{ij}, V_{s30,i}, \ldots)} + \sigma_{ij}\epsilon_{ij} + \tau_j\eta_j \tag{1}$$

where $\overline{\ln Y(M_j, R_{ij}, V_{s30,i}, \ldots)}$ is the predicted mean log ground motion intensity at location i, given an earthquake of magnitude M_j at a distance of R_{ij}, observed at a site with average shear wave velocity down to $30m$ of $V_{s30,i}$. Variability in ground motion intensity about this mean value is represented by σ_{iq} and τ_q, the within- and between-event standard deviations, respectively. The index j indicates the ground-motion intensity map ($j = 1, \ldots, m$ where $m = Q \times b$), ϵ_{ij} is a normalized within-event residual representing location-to-location variability and η_j is the normalized between-event residual. Both ϵ_{ij} and η_j are normal random variables with zero mean and unit standard deviation. The vector of ϵ_{ij} has a multivariate normal distribution and η_j is univariate.

The result is a set of m ground-motion intensity maps (e.g., Figure 2a). Since we simulate an equal number (b) of ground-motion intensity maps per earthquake scenario, the annual rate of occurrence for the j^{th} ground-motion intensity map is the original rate of occurrence of the earthquake scenario, divided by b. We denote the occurrence rate of the j^{th} ground-motion intensity map as w_j.

2.1.2. Implementation

To generate a stochastic catalog of ground-motion intensity maps, we use the OpenSHA Event Set Calculator [28]. This software outputs the mean, $\overline{\ln Y_{ij}}$, and standard deviation values, σ_{ij} and τ_j, for all locations of interest for a specified seismic source model and ground-motion prediction equation, which are needed inputs for Equation 1. The intensity measure is the 5%-damped pseudo absolute spectral acceleration (Sa) at a period $T = 1s$, which is the required input to the fragility functions below. This spectral acceleration value represents the maximum acceleration over time that a linear oscillator with 5% damping and a period of $1s$ will experience from a given ground motion. We calculate these values at the location of each component (i.e., bridges and other structures). Using one ground-motion intensity measure per component is a common simplification that facilitates the use of fragility functions to easily predict damage to a given type of structure [e.g., 29, 9]. We use the UCERF2 seismic source model to specify occurence rates of potential earthquakes in the region [30], the Wald and Allen topographic slope model to infer $V_{s30,i}$ at each location [31], the Boore and Atkinson [20] ground-motion prediction equation and the Jayaram and Baker model [27] for spatial correlation of ϵ_{ij} values.

2.2. Damage maps

2.2.1. Theory

The link between ground-motion intensity and damage to network components is provided by fragility functions. Fragility functions express the probability $P(DS_i \geq ds_\varsigma | Y_{ij} = y)$, where DS_i is a discrete random variable representing the damage state for the i^{th} component and ds_ς is a damage state threshold of interest. The damage state is conditioned on the ground motion intensity Y_{ij} having value y. We assume one component per location, and so identify both components and locations via the index i. Researchers have calibrated fragility functions using historical post-earthquake

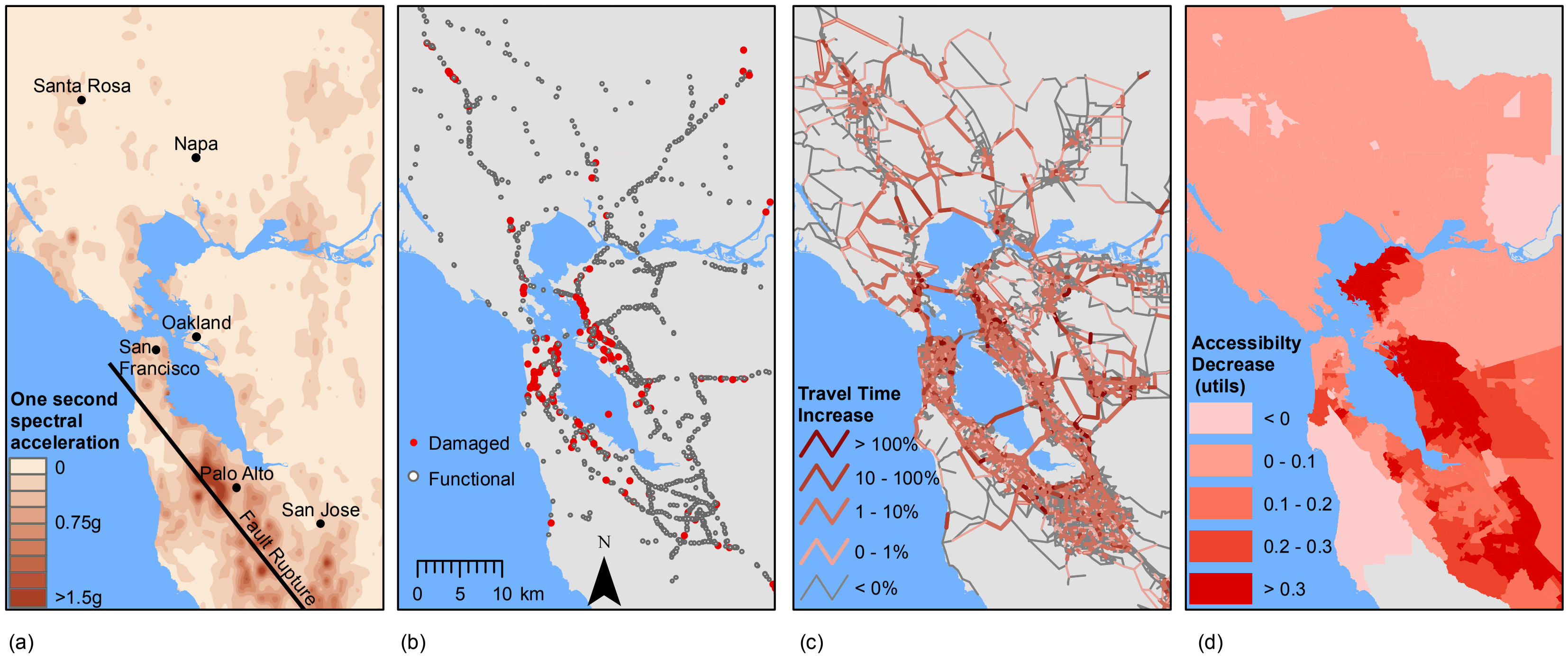

Figure 2. Illustration of the risk framework for one earthquake event including a) earthquake rupture and one-second spectral acceleration (ground motion intensity) map, b) bridge (component) damage map, c) map of travel time increase (network-performance measure) values and d) map of average accessibility decrease per travel analysis zone.

data [e.g., 32], experimental and analytical results [e.g., 33], hybrid approaches, and expert opinion. Other work has investigated correlated damage states [e.g., 34].

By sampling a damage state for each component, with probabilities obtained from the fragility functions given the ground-motion intensity, we produce a damage map (e.g., Figure 2b). The sampling process can be repeated to simulate multiple damage maps per ground-motion intensity map. For example, if c damage maps are sampled per ground-motion intensity map, the occurence rates associated with the j'^{th} damage map should be adjusted accordingly to $w_{j'}$, where $w_{j'} = w_j/c$, and $j' = 1, \ldots, J$.

Functional percentage relationships link the component damage to the functionality of network elements. For example, in a road network, when a bridge collapses, the traffic flow capacity of the road it carries and it crosses are reduced to zero. These relationships are typically derived from a combination of observation and expert opinion, often due to data scarcity [35]. Furthermore, the relationships are typically deterministic for a certain component damage state and restoration time [35]. Thus, in this paper, each damage map corresponds to a functionality state for every element of the network.

2.2.2. Implementation

Component damage. We use fragility functions of the following form to provide the link between ground-motion shaking and component damage:

$$P(DS_i \geq ds_\varsigma | Y_{ij} = y) = \Phi\left(\frac{\ln y - \lambda_{\varsigma,i}}{\xi_{\varsigma,i}}\right), \tag{2}$$

where Φ is the standard normal cumulative distribution function, $\lambda_{\varsigma,i}$ and $\xi_{\varsigma,i}$ are respectively the mean and standard deviation of the $\ln Y_{ij}$ value necessary to cause the ς^{th} damage state to occur or be exceeded for the i^{th} component, and the other variables are defined above.

The California Department of Transportation (Caltrans) provided the fragility function values $\lambda_{\varsigma,i}$ and $\xi_{\varsigma,i}$ used in this study [36]. The $\lambda_{\varsigma,i}$ values are based on bridge characteristics including number of spans and age [32], and the $\xi_{\varsigma,i}$ values are constant for all bridges. The BART seismic safety group provided the fragility function values $\lambda_{\varsigma,i}$ and $\xi_{\varsigma,i}$ used in this study for the BART-related components [37]. Data is available for the aerial structures, primarily in the East Bay, but not tunnels. The BART fragility function values correspond to the safety performance goals under the recent retrofit program, and both the $\lambda_{\varsigma,i}$ and $\xi_{\varsigma,i}$ vary depending upon the structure's characteristics. Both sets of fragility functions are based on the assumption that damage can be reasonably accurately estimated by the ground motion intensity at each site independently, and that the damage state can be reasonably estimated by an analytical model considering a single ground-motion intensity measure. In addition, the fragility curves do not directly consider the effects of degradation. Current work is ongoing to refine these assumptions [e.g., 33, 38, 39].

Per ground-motion intensity map, we sample one damage map (e.g., Figure 2b), which has a realization of the component damage state at each component location according to the fragility function (eq. 2).

Transit network damage. Each of the 43 transit systems we considered will be impacted differently. For Caltrain, conversations with managers suggest that given that there is one shared track system, the system would either be fully operational or not at all. Similarly, managers suggested modeling the VTA system as fully functional or not. Depending on where the BART train cars are when the earthquake strikes, the agency could accommodate different emergency plans. However, BART representatives suggested considering that if any part of a route is damaged, the entire corresponding route would not be operational (but other routes on different tracks might be still operational). In other words, each BART route as well as the Caltrain and VTA routes are each a weakest-link system, so the failure of a single component will cause the route to be non-operational. We modeled the ferry systems as fully functioning for all earthquake events. For all earthquake events including the baseline, trans-bay and cross-county bus lines were discontinued, but main lines in urban areas as well as other local bus networks were maintained per recommendations from the MTC (though they face delays due to modeled traffic congestion).

Road network damage. The damage state of each Caltrans bridge maps directly to the traffic capacity on associated road segments. Based on discussions with Caltrans, we consider travel conditions one week after an earthquake, since it is a critical period for decision making (for example, bridges would have been inspected and surface damage repaired, but major reconstruction would not have yet begun). According to our functional percentage relationship, at this point in time, the components are assumed to have either zero or full traffic capacity [35]. We can thus summarize the component damage using two damage states, $ds_{damaged}$ (corresponding to HAZUS *extensive* or *complete* damage states) and $ds_{functional}$ (*none*, *slight*, or *moderate* damage states) [35]. Thus, the functional percentage relationship assigns zero traffic capacity on road segments that have at least one component in the $ds_{damaged}$ damage state, and full traffic capacity otherwise.

2.3. Network performance

2.3.1. Theory

The final step for the event-based risk analysis is to evaluate the network performance measure, X. For this application, we consider a metric popular in urban planning, *mode-destination accessibility change* [e.g., 15, 41, 42] (e.g., Figure 2d). Mode-destination accessibility, hereafter referred to as accessibility, measures the distribution of travel destination opportunities weighted by the composite utility of all modes of travel to those destinations (i.e., the ease of someone getting to different destinations weighted by how desirable those destinations are) [16, 14]. The utility function for the mode-destination choice may be estimated using a multinomial random utility model where the logsum represents the accessibility value [43, 16, 14]. Namely, accessibility for a particular agent a is

$$Acc_a = \ln\left[\sum_{\forall \in C_a} \exp(V_{a(c)})\right] \tag{3}$$

where $V_{a(c)}$ is the utility of the c^{th} choice for the a^{th} person for $a = 1, \ldots, A$, and C_a is the choice set for the a^{th} person [16]. Choices refer to travel destinations and the mode of travel (driving, walking, bus, etc.). The units are a dimensionless quantity, *utils*, but can be converted into equivalent time and dollar amounts using *compensating variation* for cost-benefit studies. For the case study, 1 *util* equals the value of 75 minutes or \$20 per person per day [14, 44, 45, 46]. With nearly 7 million people in the region, even small changes in average *utils* lead to large economic losses. Since accessibility measures how easily people can get to the destinations they desire, accessibility is used as one of the measures of human welfare [e.g., 14].

Once the accessibility network performance measure is computed for each damage map, we aim to estimate the exceedance rate of different levels of performance. The annual rate, λ, of exceeding some threshold of network performance is estimated by summing the occurrence rates of all damage maps in which the performance measure exceeds the threshold:

$$\lambda_{X \geq x} = \sum_{j'=1}^{J} w_{j'} \mathbb{I}(X_{j'} \geq x) \tag{4}$$

where x is an accessibility value threshold of interest and $X_{j'}$ is the accessibility value realization for the j'^{th} damage map. The variable $w_{j'}$ is the occurrence rate of the j'^{th} damage map.The indicator function $\mathbb{I}$ evaluates to 1 if the argument, $X_{j'} \geq x$, is true, and 0 otherwise. By evaluating λ at different threshold values, we derive an exceedance curve.

2.3.2. Implementation

We compute accessibility using *Travel Model One* (version 0.3), an activity-based model used by the Metropolitan Transportation Commission (MTC), the local metropolitan planning organization (MPO) [47]. It represents the full road network as well as the public transit networks, biking, and walking. Travel demand data consists of the locations of different households in the case study area, their destination preferences and utilities, their number of vehicles, and their income and other demographic data [47, 45]. More details can be found in [48]. This data was collected by the MTC from surveys and census information. We assume that the distributions of travel preferences do not change after an earthquake, although the actual destinations and trips will vary as people choose to forgo trips due to network disruption. The result is a variable-travel-demand model. This model uses a combination of Java code called CT-RAMP [49], and the Citilabs Cube Voyager and Cube Cluster transportation planning software [47]. The software takes 6+ hours on a high-performance computing platform to analyze a given network state, including reaching equilibrium on users trip choices and prefered travel modes and routes.

Given the computational cost of analyzing the network, analyzing thousands of scenarios with a crude Monte Carlo approach is not feasible. This analysis uses an improved sampling strategy to select damaged networks for analysis,

Table 1. Income class definitions for the case study region, as defined by the local planning organization, the MTC [45] and also translated to current 2014 USD using the consumer price index.

Income class	Income range, 1989 USD	Income range, 2014 USD
Low	0 - $25,000	0 - $47,334
Medium	$25,000 - $45,000	$47,334 - $85,202
High	$45,000 - $75,000	$85,202 - $142,004
Very high	more than $75,000	more than $142,004

and considers 40 sets of ground-motion intensity maps, damage maps, accessibility performance measure realizations, and corresponding annual rates of occurrence. The 40 realizations were selected (and their occurence rates adjusted appropriately) using an optimization procedure to ensure that the selected scenarios were consistent with the larger original set of simulations, in terms of the probability distributions of ground motion intensity at individual sites, and other parameters that ensured reasonableness of the distributions of network damage. In this sense, the selected simulations are a "hazard consistent" representation of the distribution of future earthquake impacts that could be experienced in the region. Readers are referred to [17] for more details about this set of events, and further details about computing mode-destination accessibility using this model.

3. Results and discussion

3.1. Region-wide results

In this section, we analyze region-wide trends in accessibility losses for the case study area. We first analyze each of the 12 socio-economic groups used in practice for the case study region [45]. These socio-economic groups correspond to all combinations of four income classes (Table 1), and three classes of automobile availability in the household (zero automobiles, fewer automobiles than household members that work, as many or more automobiles than household members that work). Each data point for analysis represents a trip by a person of a household from one of these segments, who is modeled as an agent in the transportation model. Expected losses are computed by taking an average of the accessibility losses for people within a given group and region for each earthquake event, weighted by the events' corresponding occurrence rates. Expected losses for people from each of the 12 groups and 1454 TAZs are shown in Figure 3.

In addition to looking at average accessibility loss, we can compute an accessibility exceedance curve for a given group or region. By using equation 4 to compute exceedance rates for multiple accessibility loss thresholds, we can produce results like those in Figure 4. These curves show, for a given group, the annual rate with which a given accessibility decrease will be observed (when considering random future occurrences of earthquakes and damage). Several observations can be made from these results.

First, a higher ratio of cars to the number of people who work in a household corresponds to a higher expected decreases in accessibility (as seen by looking across a column in Figure 3). Households with more cars tend to take longer trips, and there is a relationship between needing to travel longer distances and needing an extra cars in a household. But there is only a weak trend between average trip length for a TAZ and the predicted impact on accessibility (Figure 5). Instead, we hypothesize that there are other latent variables correlated with both car ownership and accessibility risk (such as geographic location). In Section 3.5, we will further explore the relationship between the percentage of car-based trips and accessibility risk.

Second, controlling for car ownership, we see a fairly consistent distribution of risk across income classes. For example, looking at households with fewer workers than cars (the middle column of Figure 3), the variation from TAZ to TAZ is much greater than the difference across income segments. Similarly, while trip lengths are slightly longer for higher income households, the differences are subtle. Thus, for a given TAZ, the differences in impacts across incomes are not that great. There is, however, an unequal geographic distribution of wealth in the study region. Because of this, when we aggregate accessibility risk across TAZs, we see that accessibility risk rises slightly with increasing household income (Figure 4b).

Next, we consider TAZs indicated to have elevated risk: due east of San Francisco, in the suburbs of San Jose, along the coastal and bay-side regions south of San Francisco (e.g., Millbrae and Pacifica), and in parts of San

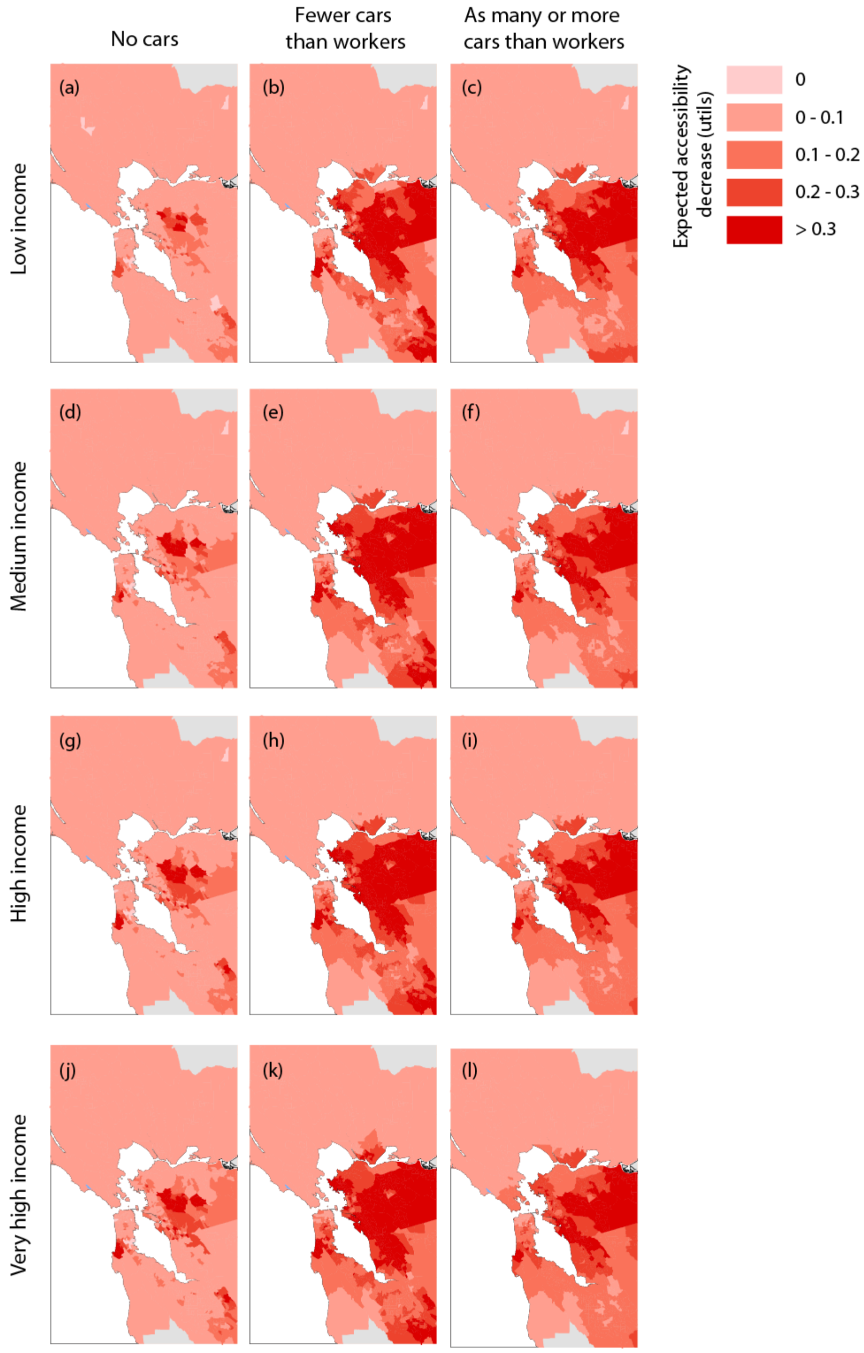

Figure 3. Expected changes in accessibility per person per day for each combination of income class and car ownership group. The darker the color, the greater the losses in accessibility. Each row of figures corresponds to an income class and each column corresponds to a class of car ownership).

Francisco (south-central neighborhoods including the Westland Highlands and Glen Park neighborhoods). Geographic proximity to hazardous faults is one source of spatial variation. The San Francisco Peninsula is at risk of disruption from large magnitude San Andreas earthquakes, while the East Bay is at risk from slightly smaller but more frequent events on the Hayward Fault. Network simulations indicate that both Hayward and San Andreas earthquakes can

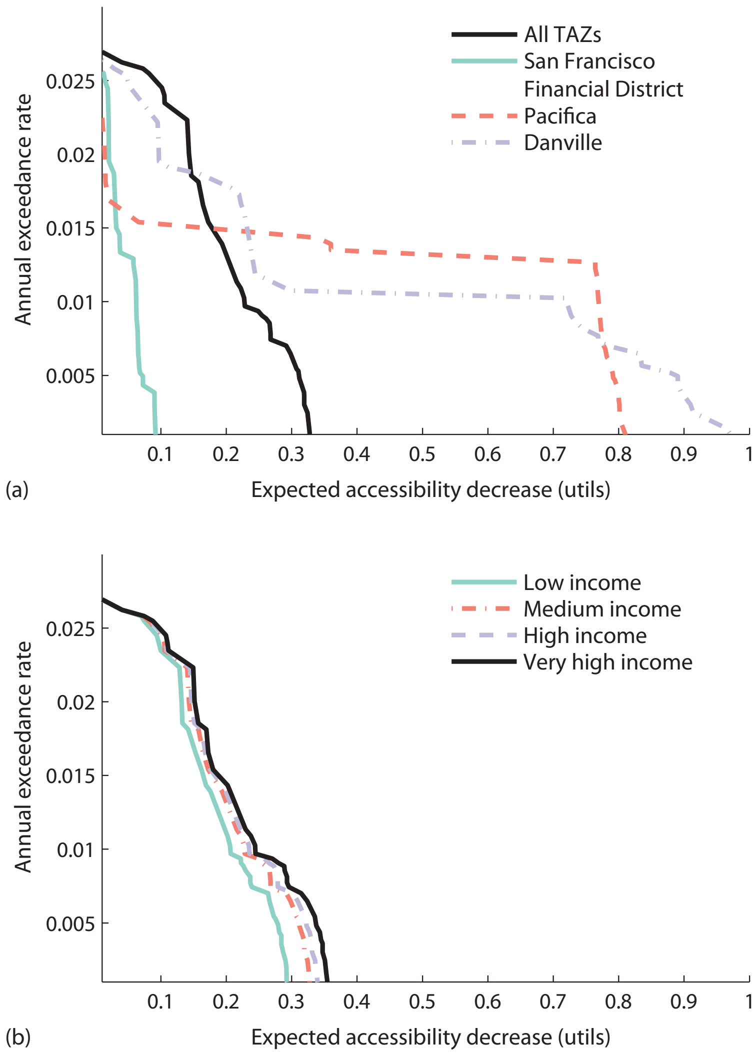

Figure 4. Accessibility annual loss exceedance curve with a comparison by (a) case study TAZs and average over all TAZs and (b) income class; all curves are for medium income households with fewer cars than workers.

cause accessibility problems for the East Bay. Figure 6 shows realizations of a magnitude 6.85 Hayward event and a magnitude 7.45 San Andreas event—both show high accessibility losses in the East Bay. In contrast, the main predicted accessibility losses in San Francisco correspond primarily to San Andreas events. Figures 6c and 6d provide one such example. Figures 6e and 6f show a lower magnitude event farther away from the main population centers: a magnitude 6.35 event in the Great Valley Pittsburg-Kirby Hills Fault. This shows how the more minor faults in the East Bay can contribute to that area's risk. The Figure 6 results are for one specific socio-economic group, but comparable results for the other groups show the same general patterns.

Finally, we can examine the rates of loss exceedance (eq. 4), as shown in Figure 4. Recognizing that the impact varies significantly by TAZ, as indicated by Figure 3, we also examine the accessibility loss exceedance curve for three communities: part of the San Francisco Financial District, Danville, and Pacifica. This part of the San Francisco Financial District represents an area with relatively low expected changes in accessibility, whereas Danville and Pacifica are at an elevated risk in almost all socio-economic groups (Figure 3). The general trends are corroborated by

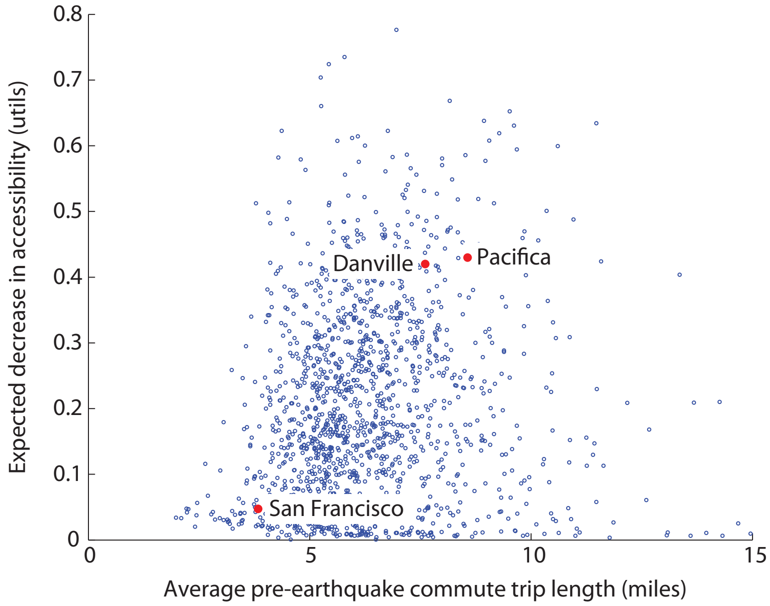

Figure 5. Average pre-earthquake trip length versus change in expected accessibility for all TAZs in the study region. Each dot represents data from one TAZ, and red dots highlight the data points for the three case study communities.

the loss exceedance curves for these three communities (Figure 4a shows results for medium income households with fewer cars than workers). The average middle-class person from Danville in a household with fewer cars than workers is expected to experience travel-related losses up to 1 *util* (or 75 minutes of extra travel time per day) after a rare earthquake. In contrast, a resident of San Francisco's Financial District has expected losses of only a tenth as much when considering the same exceedance rate. At annual rates of less than 0.01 (i.e., return periods greater than 100 years), Danville and Pacifica follow a similar general pattern, which differs dramatically from that of San Francisco.

3.2. Analysis for San Francisco Financial District

Two factors might explain why this San Francisco TAZ has lower expected accessibility losses than most other communities. First, it differs dramatically from many other TAZs in having a small percentage of trips made by car (38% versus an average of 85% across all TAZs). Households traveling by foot or bike are less influenced by network damage, because foot travel routes and travel times will are not affected by damage in this model. Additionally, trips by foot and bike tend to be to destinations that are shorter distances away than trips made via other modes. Second, the times for trips to and from work are similar to that of other TAZs, and the average trip distance is only 7% lower than the average for all trips region-wide. So the trip times and lengths do not explain the differences in accessibility losses in this TAZ. The data thus suggests that a major cause for the areas low accessibility risk is the low dependence on cars for mobility.

3.3. Analysis for Pacifica

We might not anticipate Pacifica to be at high risk of accessibility losses compared to other similar communities close to earthquake faults. The percentage of pre-earthquake car-based trips is around average for the case study area (88% versus an average of 85%). In contrast to most other regions, however, Pacifica is wedged between the Pacific Ocean to the west and the coastal mountains to the east. The main access road is historic California Highway 1, which has a number of older vulnerable bridges. There are no viable alternative routes on local roads. Almost all trips from Pacifica are taken by car, and the average trip length is 108% longer than the region-wide average, the Highway 1 vulnerability is particularly serious.

As a comparison, consider Half Moon Bay, a community about 13 miles to the south (Figure 7). Half Moon Bay has significantly lower expected accessibility losses compared to Pacifica (0.11 *utils* for a middle income household

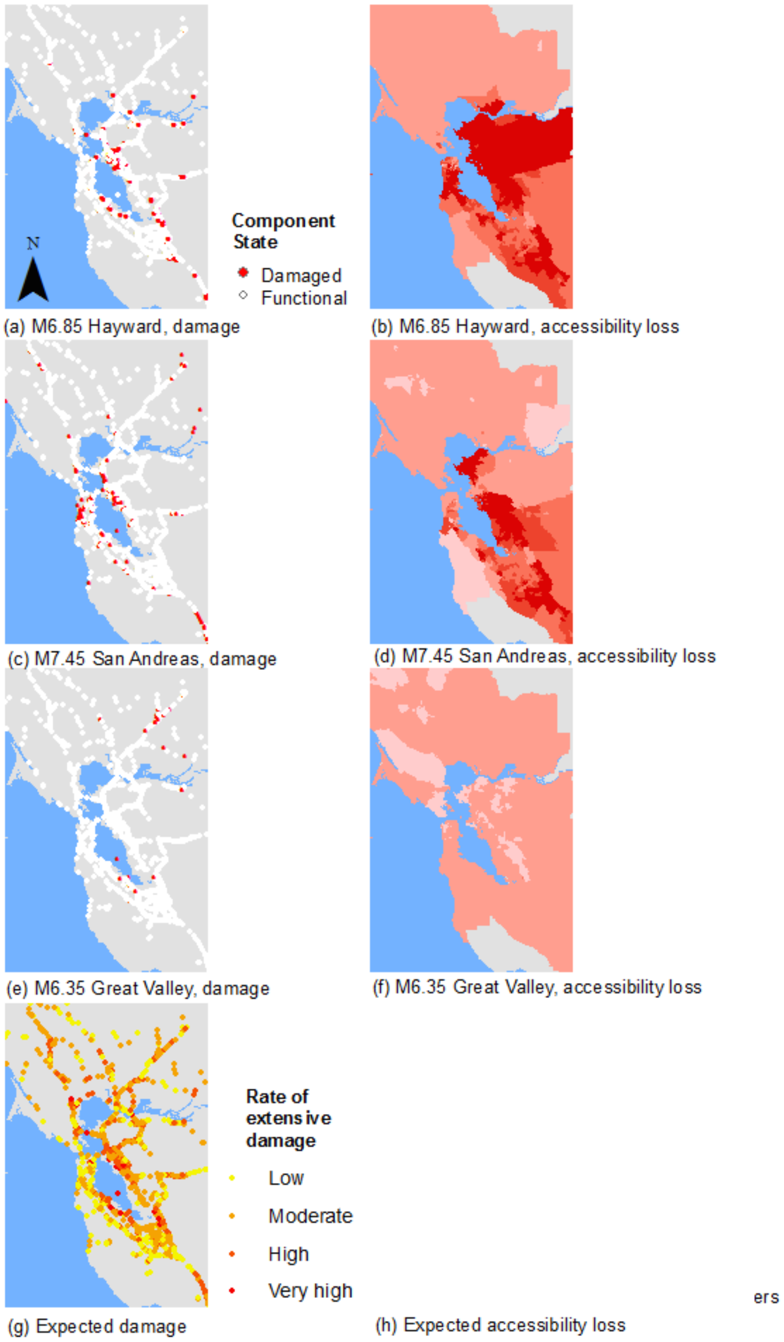

Figure 6. Bridge damage and corresponding accessibility losses by TAZ for medium income households with fewer cars than workers. The top three rows show results from specific events, while the bottom row has expected values calculated as a weighted average over all events. **TODO: clean up figure**

with fewer cars than workers, versus 0.43 *utils* in Pacifica). While the seismic hazard for the two towns is similar, Half Moon Bay's population is about one third of Pacifica's, so there is less local demand for Highway 1's limited road capacity [51]. Furthermore, and likely most significantly, Half Moon Bay has a key alternative to California Highway 1, California Highway 92, which links to Silicon Valley and the main highways of that region (US-101 and

I-280). Since Pacifica is unusually reliant on one road with key vulnerabilities, it has an elevated risk for losses in accessibility.

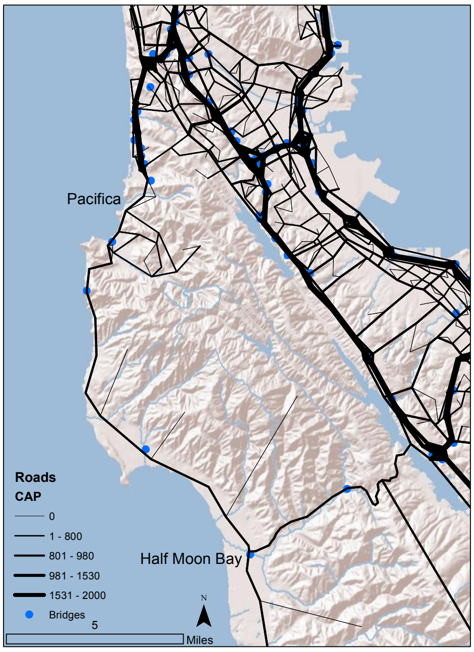

Figure 7. Roads providing access from Pacifica and Half Moon Bay **TODO: label Highway 1 and Highway 92, clean up legend.**

3.4. Analysis for Danville

Pre-earthquake commute trips from Danville are on average longer in distance and duration than the previous communities. The average length of a trip from Danville is 85% longer than the average over all trips in the study region. More specifically, there is a relatively higher proportion of trips taking 60-74 minutes and traveling over 40 miles than in the previous communities. These longer trips have more opportunities to be impacted by road closures, because more roads and bridges will be used to complete the trip. Moreover, the road layout near Danville mandates many highway trips, which increase the likelihood of crossing (damage prone) bridges.

Bridge damage is important for many regions, including Danville, because the percentage of car-based trips is high (85% of all trips from Danville). For all three simulations shown in Figure 6, some bridges in the Oakland area are damaged and thsu closed. In addition, in the first two simulations, there are closures to the north of Danville, which represents one of the two main travel routes from Danville. There are also scattered closed bridges to the west of Danville, a top travel corridor for people of Danville because of the workplace centers in San Francisco, Oakland, and Silicon Valley (all to the west). As for transit, in the first two events, all BART lines are closed, so there are limited alternatives to the popular road routes. The result is that the residents of Danville have reduced access to their normal destinations after all these events. Looking at the rate of bridge damage across all of the earthquake simulations in Figure 6g, we see that bridges in the Oakland-Berkeley area and to the north of Danville are particularly likely to be damaged. This suggests that Danville's proximity to vulnerable bridges contributes to its accessibility risk.

3.5. Impact of travel mode shifts and regional variations in travel mode patterns

First, we compare patterns of transit system damage with patterns of travel mode shifts after earthquake events. Over all the simulated events, taking a weighted average by the annual occurrence rate of each event, we see a 25%

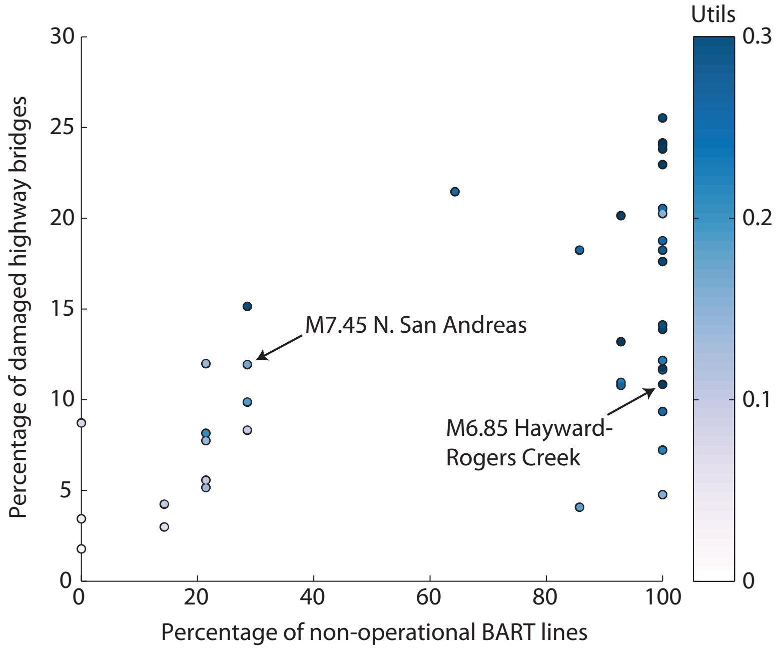

Figure 8. Percentage of BART lines not operational versus percentage of highway bridges damaged, where each data point corresponds to one earthquake simulation. The points are color-coded by the average loss in accessibility per day per person over all TAZs for households with the fewer cars than workers.

Table 2. Number of the 40 earthquake realizations in which for major transit networks have a specified level of functionality. Functionality is measured by the percentage of lines that are operational in a given realization.

Functionality	BART	Caltrain	Muni Light Rail	VTA Light Rail
Full	3	13	25	9
50-99%	10	0	15	0
1-49%	8	0	0	0
None	19	27	0	31

reduction in transit ridership after an earthquake. The heavy rail systems (BART and Caltrain) are not fully operational in most of the forty simulated events (Table 2), and these have heavy ridership. The light rail systems (VTA and Muni) also suffer losses in many events (Table 2). Some of the pre-earthquake transit trips do not take place at all in the post-earthquake simulations, and some switch to other modes (foot, car, and bike), causing small average increases in the number of trips taken by other modes. One exception to this trend is the M6.35 Great Valley, Pittsburg-Kirby Hills Fault earthquake event, illustrated in Figure 6e and 6f. In this event, there were no line closures on the four major transit systems listed in Table 2. There were, however, some bridge closures on the highways, resulting in a slight increase in transit ridership and also in trips by foot.

In general, accessibility impact grows with increasing number of damaged transit lines, particularly in combination with high numbers of damaged bridges (Figure 8). Individual network simulations also suggest that transit is a key contributor to accessibility risk. For example, the M6.85 Hayward Rogers-Creek and the M7.45 Northern San Andreas Fault events from Figure 6 both have around 11% of bridges damaged. These events are labeled in Figure 8, which indicates that the Hayward Rogers-Creek event has significantly higher transit network damage and accessibility loss. The Northern San Andreas event had 10 of the 14 BART lines and all Muni lines operational, whereas the Hayward Rogers-Creek event had no BART lines and 5 of the 8 Muni lines operational (Caltrain and VTA were not operational in either simulation). Moreover, the differences in accessibility results could not have been predicted from simpler models focusing on bridge portfolio losses, because the percent of damaged bridges was about the same, and the San Andreas event actually corresponded to a greater increase in fixed-demand travel time when modeled using a much simpler traffic model.

Next, we examine the correlation between a community's walkability, as measured by the percentage of total trips made by that travel mode, and its expected decrease in accessibility. Figure 9 shows that communities with a high percentage of pre-earthquake trips on foot have a lower average decrease in accessibility. This result corroborates the specific example of the San Francisco Financial District discussed in Section 3.2. Furthermore, on average, the number of by-foot trips increases after the earthquake events where road congestion worsens. This model result is consistent with the observations after the 1995 Kobe earthquake, in which many commuters switched to walking and biking in the weeks after the earthquake [7]. This suggests that communities with greater walkability are also more resilient to earthquake-related accessibility risk.

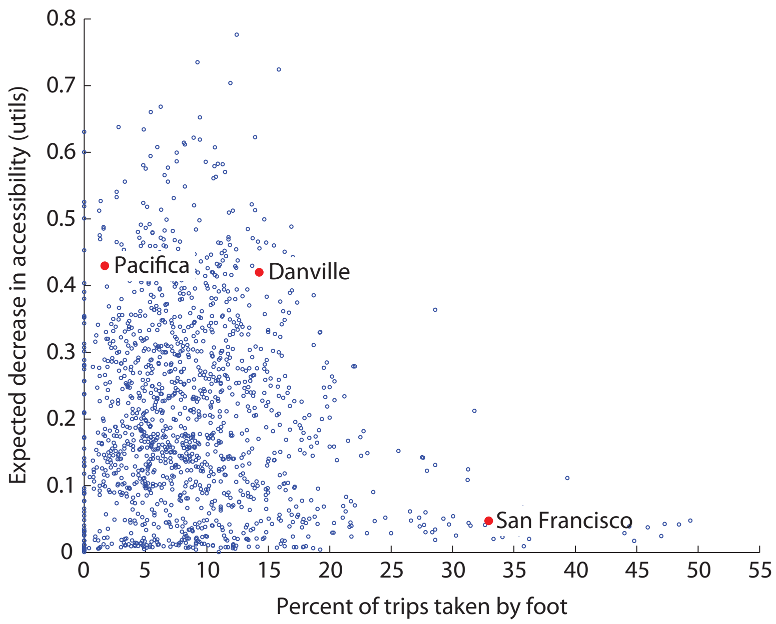

Figure 9. Percentage of pre-earthquake trips taken by foot versus expected decrease in accessibility among households with fewer cars than workers, for all TAZs in the study area. Each dot represents data from one TAZ, and red dots highlight the data points for the three case study communities.

4. Conclusions

We have shown how mode-destination accessibility can be used to link post-earthquake infrastructure damage to the impact on human welfare and enables identifying at-risk geographic and demographic groups in a region. Adopting this state-of-the-art performance metric from the urban planning community, we have illustrated its use for seismic risk assessment and mitigation through a case study of the San Francisco Bay Area. For the case study, we considered a set of 40 hazard-consistent earthquake scenarios, ground-motion intensity maps, damage maps, and corresponding annual rates of occurrence. For each damage map, we performed a detailed activity-based travel model calculation that includes the road network, transit networks, walking and biking options, variable travel demand, and mode choice. We used this data and model to compute the mode-destination accessibility, a performance measure for each community and each socio-economic group (defined by income class and car ownership).

We saw stark differences in accessibility from location to location. The far East Bay, south San Jose and some communities south of San Francisco were particularly at risk. We found that these geographic trends persisted across income classes and car ownership groups. Nonetheless higher income households with more cars than workers had higher average accessibility losses than other socio-economic groups. One key reason is the geographic clustering of these households in higher-risk areas. Another factor is that these households tend to take longer daily trips, thus crossing more roads and bridges and possibly increasing the likelihood of disruption.

This study also demonstrated that travel modes shift after an earthquake, and communities that can more easily adjust are predicted to experience lower post-earthquake losses in accessibility. The results suggest that the walkability of a community, as measured by the percentage of pre-earthquake trips by foot, is closely linked to reduced accessibility risk. We also found that in almost all of the simulated earthquake events, the transit system is predicted by this model to be severely impacted. The result is a reduced mode share for transit and increased trips by the other modes (car, walking, and bike). Thus, this study suggests that not modeling transit disruption can lead to a nonconservative estimate of seismic risk of transportation systems. The model shows, however, that when transit is not damaged—which is very rare for this case study—ridership increases.

In conclusion, mode-destination accessibility offers important insights into the relationship between damage to physical infrastructure and impacts on human welfare. Using a detailed transportation network model, computationally efficient analysis strategies, and this refined measures of impact, we obtain new insights about users' risk, and obtain metrics that are usable by urban planners responsible for long-term management of transportation systems. This approach provides a foundation for future work in risk mitigation and policy to reduce the vulnerability of at-risk communities. It suggests that initiatives making communities more conducive for cycling and walking to work can increase resiliency to disasters. It also provides a method to quantify societal benefits of upgrading various aspects of a regions' transportation systems.

5. Acknowledgements

We thank Dave Ory at the Metropolitan Transportation Commission (MTC) and Tom Shantz and Loren Turner at Caltrans for motivating discussions and providing the case study data. The first author thanks the support of the NSF and Stanford Graduate Research Fellowships. This work was supported in part by the National Science Foundation under NSF grant number CMMI 0952402. Any opinions, findings and conclusions or recommendations expressed in this material are those of the authors and do not necessarily reflect the views of the National Science Foundation.

References

[1] L. Dueñas-Osorio, J. I. Craig, B. J. Goodno, Seismic response of critical interdependent networks, Earthquake Engineering & Structural Dynamics 36 (2) (2007) 285306. doi:10.1002/eqe.626.

[2] S. E. Chang, M. Shinozuka, J. E. Moore, Probabilistic earthquake scenarios: Extending risk analysis methodologies to spatially distributed systems, Earthquake Spectra 16 (3) (2000) 557–572. doi:10.1193/1.1586127.

[3] R. C. Bolin, L. Stanford, The Northridge earthquake: vulnerability and disaster, Routledge, London; New York, 1998.

[4] The World Bank and the United Nations, Natural hazards, unnatural disasters: the economics of effective prevention, Tech. rep., The World Bank, Washington D.C. (2010).

[5] California. Dept. of Transportation. Post Earthquake Investigation Team, Northridge earthquake, 17 January 1994: PEQIT report, California Department of Transportation, Division of Structures, Sacramento, 1994.

[6] K. J. Tierney, Business Impacts of the Northridge Earthquake, Journal of Contingencies and Crisis Management 5 (2) (1997) 87–97. doi:10.1111/1468-5973.00040.

[7] P. Gordon, H. W. Richardson, B. Davis, Transport-related impacts of the Northridge earthquake, National Emergency Training Center, 1998.

[8] A. Kiremidjian, J. Moore, Y. Y. Fan, O. Yazlali, N. Basöz, M. Williams, Seismic risk assessment of transportation network systems, Journal of Earthquake Engineering 11 (3) (2007) 371–382. doi:10.1080/13632460701285277.

[9] N. Jayaram, J. W. Baker, Efficient sampling and data reduction techniques for probabilistic seismic lifeline risk assessment, Earthquake Engineering & Structural Dynamics 39 (10) (2010) 1109–1131. doi:10.1002/eqe.988.

[10] C. S. Oliveira, M. A. Ferreira, F. M. d. S, The concept of a disruption index: application to the overall impact of the July 9, 1998 Faial earthquake (Azores islands), Bulletin of Earthquake Engineering 10 (1) (2012) 7–25. doi:10.1007/s10518-011-9333-8.

[11] P. Bocchini, D. M. Frangopol, Restoration of bridge networks after an earthquake: Multicriteria intervention optimization, Earthquake Spectra 28 (2) (2012) 426–455. doi:10.1193/1.4000019.

[12] F. Cavalieri, P. Franchin, P. Gehl, B. Khazai, Quantitative assessment of social losses based on physical damage and interaction with infrastructural systems, Earthquake Engineering & Structural Dynamics 41 (11) (2012) 1569–1589. doi:10.1002/eqe.2220.

[13] F. S. Chapin, Urban land use planning, University of Illinois Press, 1970.

[14] D. A. Niemeier, Accessibility: an evaluation using consumer welfare, Transportation 24 (4) (1997) 377396.

[15] K. T. Geurs, B. van Wee, Accessibility evaluation of land-use and transport strategies: review and research directions, Journal of Transport Geography 12 (2) (2004) 127–140. doi:10.1016/j.jtrangeo.2003.10.005.

[16] S. L. Handy, D. A. Niemeier, Measuring accessibility: an exploration of issues and alternatives, Environment and Planning A 29 (7) (1997) 11751194.

[17] M. Miller, Seismic risk assessment of complex transportation networks, PhD thesis, Stanford University (2014).

[18] M. Miller, J. Baker, Ground-motion intensity and damage map selection for probabilistic infrastructure network risk assessment using optimization, in review (2014).

[19] R. Cervero, K.-L. Wu, Polycentrism, commuting, and residential location in the San Francisco Bay area, Environment and Planning A 29 (5) (1997) 865–886.

[20] D. M. Boore, G. M. Atkinson, Ground-motion prediction equations for the average horizontal component of PGA, PGV, and 5%-damped PSA at spectral periods between 0.01 s and 10.0 s, Earthquake Spectra 24 (1) (2008) 99–138.

[21] N. Abrahamson, W. Silva, Summary of the Abrahamson & Silva NGA Ground-Motion Relations, Earthquake Spectra 24 (1) (2008) 67–97. doi:10.1193/1.2924360.

[22] B. Chiou, R. R. Youngs, An NGA model for the average horizontal component of peak ground motion and response spectra, Earthquake Spectra 24 (1) (2008) 173–215. doi:10.1193/1.2894832.

[23] K. W. Campbell, Y. Bozorgnia, NGA ground motion model for the geometric mean horizontal component of PGA, PGV, PGD and 5% damped linear elastic response spectra for periods ranging from 0.01 to 10s, Earthquake Spectra 24 (1) (2008) 139–171. doi:10.1193/1.2857546.

[24] J. W. Baker, C. A. Cornell, Which spectral acceleration are you using?, Earthquake Spectra 22 (2) (2006) 293–312. doi:10.1193/1.2191540.

[25] R. Foulser-Piggott, P. J. Stafford, A predictive model for Arias intensity at multiple sites and consideration of spatial correlations, Earthquake Engineering & Structural Dynamics 41 (3) (2012) 431451. doi:10.1002/eqe.1137.

[26] Y. Han, R. A. Davidson, Probabilistic seismic hazard analysis for spatially distributed infrastructure, Earthquake Engineering & Structural Dynamics 41 (15) (2012) 2141–2158. doi:10.1002/eqe.2179.

[27] N. Jayaram, J. W. Baker, Correlation model for spatially distributed ground-motion intensities, Earthquake Engineering & Structural Dynamics 38 (15) (2009) 1687–1708. doi:10.1002/eqe.922.

[28] E. H. Field, T. H. Jordan, C. A. Cornell, OpenSHA: a developing community-modeling environment for seismic hazard analysis, Seismological Research Letters 74 (4) (2003) 406 – 419. doi:10.1785/gssrl.74.4.406.

[29] M. Shinozuka, Y. Murachi, X. Dong, Y. Zhou, M. J. Orlikowski, Effect of seismic retrofit of bridges on transportation networks, Earthquake Engineering and Engineering Vibration 2 (2) (2003) 169–179. doi:10.1007/s11803-003-0001-0.

[30] E. H. Field, T. E. Dawson, K. R. Felzer, A. D. Frankel, V. Gupta, T. H. Jordan, T. Parsons, M. D. Petersen, R. S. Stein, R. J. Weldon, C. J. Wills, Uniform California Earthquake Rupture Forecast, Version 2 (UCERF 2), Bulletin of the Seismological Society of America 99 (4) (2009) 2053 –2107. doi:10.1785/0120080049.

[31] D. J. Wald, T. I. Allen, Topographic slope as a proxy for seismic site conditions and amplification, Bulletin of the Seismological Society of America 97 (5) (2007) 1379–1395. doi:10.1785/0120060267.

[32] N. Basöz, J. Mander, Enhancement of the highway transportation lifeline module in HAZUS, Tech. rep., Final Pre-Publication Draft (#7) prepared for the National Institute of Building Sciences (NIBS) (1999).

[33] K. N. Ramanathan, Next generation seismic fragility curves for California bridges incorporating the evolution in seismic design philosophy, PhD thesis, Georgia Institute of Technology (2012).

[34] R. Lee, A. S. Kiremidjian, Uncertainty and correlation for loss assessment of spatially distributed systems, Earthquake Spectra 23 (4) (2007) 753–770. doi:10.1193/1.2791001.

[35] S. Werner, C. Taylor, S. Cho, J. Lavoie, REDARS 2 methodology and software for seismic risk analysis of highway systems (technical manual), Tech. rep., Seismic Systems & Engineering Analysis for MCEER, Oakland, CA (2006).

[36] Caltrans, Caltrans Seismic Design Criteria Version 1.7, Tech. Rep. SDC 1.7, California Department of Transportation, Sacramento, CA (2013).

[37] Bechtel/HNTB Team, Design Criteria Volume I, Version 1.2, Tech. rep., San Francisco Bay Area Rapid Transit District, San Francisco Bay Area Rapid Transit District Earthquake Safety Program (2008).

[38] N. Kurtz, J. Song, P. Gardoni, Time-varying seismic reliability analysis of representative US west coast bridge transportation networks, in: G. Deodatis, B. R. Ellingwood, D. M. Frangopol (Eds.), Safety, Reliability, Risk and Life-Cycle Performance of Structures and Infrastructures, CRC Press, 2014, pp. 655–662.

[39] J. Ghosh, K. Rokneddin, J. E. Padgett, L. Dueas-Osorio, Seismic reliability assessment of aging highway bridge networks with field instrumentation data and correlated failures. I: Methodology, Earthquake Spectra 30 (2) (2013) 795–817. doi:10.1193/040512EQS155M.

[40] S. Pugh, Construction statistics, Tech. rep., California Department of Transportation Division of Engineering Services (2012).

[41] K. Kockelman, Travel Behavior as Function of Accessibility, Land Use Mixing, and Land Use Balance: Evidence from San Francisco Bay Area, Transportation Research Record: Journal of the Transportation Research Board 1607 (-1) (1997) 116–125. doi:10.3141/1607-16.

[42] P. Waddell, F. Nourzad, Incorporating nonmotorized mode and neighborhood accessibility in an integrated land use and transportation model system, Transportation Research Record: Journal of the Transportation Research Board 1805 (-1) (2002) 119–127. doi:10.3141/1805-14.

[43] C. F. Manski, Structural analysis of discrete data with econometric applications, MIT Press, 1981.

[44] K. A. Small, H. S. Rosen, Applied welfare economics with discrete choice models, Econometrica 49 (1) (1981) 105–130. doi:10.2307/1911129.

[45] D. Ory, Personal communication (2013).

[46] United States Department of Transportation, Revised departmental guidance: valuation of travel time in economic analysis, US Department of Transportation, Washington, DC.

[47] G. Erhardt, P. Brinckerhoff, D. Ory, A. Sarvepalli, J. Freedman, J. Hood, B. Stabler, MTC's Travel Model One: applications of an activity-based model in its first year, in: Innovations in Travel Modeling 2012, Tampa, Florida, 2012, p. 9.

[48] P. Waddell, UrbanSim: modeling urban development for land use, transportation, and environmental planning, Journal of the American Planning Association 68 (3) (2002) 297–314. doi:10.1080/01944360208976274.

[49] W. Davidson, P. Vovsha, J. Freedman, R. Donnelly, CT-RAMP family of activity-based models, in: Proceedings of the 33rd Australasian Transport Research Forum (ATRF), Canberra, Australia, 2010, p. 15.

[50] H. Wakabayashi, H. Kameda, Network performance of highway systems under earthquake effects: a case study of the 1989 Loma Prieta earthquake, in: Proceedings US-Japan Workshop on Earthquake Disaster Prevention for Lifeline Systems, 1992, pp. 215–232.

[51] U.S. Bureau of the Census, United States Census 2010, Tech. rep., U.S. Census Bureau, Washington D.C. (2010).